

Double fermionic contributions to the heavy-quark vacuum polarization

Michał Czakon^{1,2} and Thomas Schutzmeier¹

¹ *Institut für Theoretische Physik und Astrophysik, Universität Würzburg,
Am Hubland, D-97074 Würzburg, Germany*

² *Department of Field Theory and Particle Physics, Institute of Physics,
University of Silesia, Uniwersytecka 4, PL-40007 Katowice, Poland*

ABSTRACT: We compute the virtual $\mathcal{O}(\alpha_s^3 n_f^2)$ corrections to the heavy quark vector current correlator in terms of expansions in the external momentum and as an exact numerical solution. As a byproduct, the available high-energy expansion at the three-loop level is extended.

Contents

1. Introduction	1
2. Definitions	2
3. Calculation	3
4. Results	5
5. Conclusions	8

1. Introduction

Correlators of two currents, basic objects in Quantum Field Theory, provide important information for both theoretical and phenomenological applications. Depending on the Lorentz structure of the current under consideration, different interesting observables are directly related to these quantities, like the hadronic cross section in electron-positron annihilation, $R(s)$, and decay rates of Z- and Higgs-bosons.

On this account current correlators are investigated thoroughly in perturbation theory, where even high order calculations are possible. Some applications, like the determination of the charm and bottom quark masses through sum-rules carried out to four loops in [1, 2], corrections to the ρ parameter [3, 4] or the recent evaluation of α_s from low energy data at the same level of precision [5], require asymptotic expansions of heavy quark correlators in the low and/or high energy limits. Other studies, however, necessitate the knowledge of the full external momentum dependence p^2 , for instance the determination of the fine structure constant at the Z-boson mass scale, $\alpha_{\text{em}}(M_Z)$ [6].

Up to the three-loop level, all physically relevant correlators have been computed including the full quark mass dependence in [7, 8, 9] by deriving Padé approximants from asymptotic expansions. At four-loop accuracy, in the case of the vector current including one heavy quark, the first two terms in the low energy series are currently known [1, 10] and were obtained by direct Taylor expansion of all propagator-type integrals and subsequent reduction of tadpole diagrams. In the high energy limit, besides the leading massless contribution [11, 12, 13, 14, 15, 16], the first two mass correction terms of the absorptive part of the scalar, vector and axial-vector current correlators are also available [17, 18], partially even to five loops [19, 20].

Unfortunately, the techniques used to achieve these results are, due to their huge computational complexity, not suitable for the computation of higher order terms in the expansions. Thus, reconstructing the full momentum dependence at $\mathcal{O}(\alpha_s^3)$ in an analogous manner to

the three-loop case demands a completely different method. A promising and effective approach in this context is based on differential equations, originally proposed in [21, 22]. Using this technique, we were already able to compute the first 30 terms in the low energy expanded polarization function at $\mathcal{O}(\alpha_s^2)$ in [23]. Recently, these results were confirmed in [24] utilizing the same approach.

The purpose of this paper is to exploit this method and demonstrate its applicability up to the four-loop level. We compute the vacuum polarization for low and high energies as expansions up to $(p^2)^{30}$ and $(p^2)^{-15}$, respectively, and moreover the full momentum dependence in numerical form in the Euclidean and Minkowskian region. As new results, we extend the available information in the high energy domain at $\mathcal{O}(\alpha_s^2)$ and provide the double fermionic contributions to the vector current correlator at $\mathcal{O}(\alpha_s^3)$.

This work is organized as follows. In the next section we sum up the relevant notation. Computational methods are briefly presented in Section 3, whereas the first terms of the expansions and the numerical results are given in Section 4. Finally, we give our conclusions.

2. Definitions

Given the vector current $j^\mu(x) = \bar{q}_h(x)\gamma^\mu q_h(x)$ composed of the heavy quark field $q_h(x)$ with mass m , the two point correlator is defined by

$$\Pi^{\mu\nu}(p^2) = i \int dx e^{ixp} \langle 0 | T j^\mu(x) j^\nu(0) | 0 \rangle \quad (2.1)$$

where p^μ is the external momentum. A convenient representation of the tensor $\Pi^{\mu\nu}(p^2)$ through the scalar vacuum polarization function $\Pi(p^2)$ is given by

$$\Pi^{\mu\nu}(p^2) = (-p^2 g^{\mu\nu} + p^\mu p^\nu) \Pi(p^2) + p^\mu p^\nu \Pi_L(p^2). \quad (2.2)$$

Transversality of the vector current correlator requires $\Pi_L(p^2) = 0$. Through the optical theorem the aforementioned hadronic ratio $R(s)$ is related to the current correlator

$$R(s) = \frac{\sigma(e^+e^- \rightarrow \text{hadrons})}{\sigma(e^+e^- \rightarrow \mu^+\mu^-)} = 12\pi \text{Im}\Pi(p^2 = s + i\epsilon). \quad (2.3)$$

In the framework of perturbation theory, the polarization function can be expanded in the strong coupling as

$$\Pi(p^2) = Q_h^2 \frac{3}{16\pi^2} \sum_{k \geq 0} \left(\frac{\alpha_s(\mu)}{\pi} \right)^k \Pi^{(k)}(p^2). \quad (2.4)$$

Since in this work the focus is set on double fermionic contributions at $\mathcal{O}(\alpha_s^3)$ stemming from diagrams sketched in fig. 1, it is convenient to decompose $\Pi^{(3)}(p^2)$ into bosonic and fermionic contributions,

$$\begin{aligned} \Pi^{(3)}(p^2) = & C_F^3 \Pi_A^{(3)}(p^2) + C_F^2 C_A \Pi_{\text{NA},1}^{(3)}(p^2) + C_F C_A^2 \Pi_{\text{NA},2}^{(3)}(p^2) \\ & + C_F^2 T_F \Pi_{\text{sf},A}^{(3)}(p^2) + C_F C_A T_F \Pi_{\text{sf},\text{NA}}^{(3)}(p^2) \\ & + C_F T_F^2 \Pi_{\text{df}}^{(3)}(p^2), \end{aligned} \quad (2.5)$$

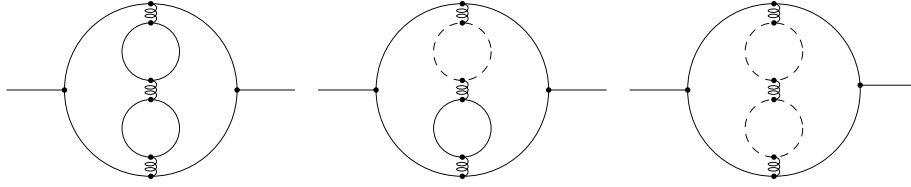


Figure 1: Diagrams contributing to $\Pi_{\text{df}}^{(3)}(p^2)$. Solid (dashed) lines refer to massive (massless) propagators.

where $\Pi_{\text{sf}}^{(3)}(p^2)$ and $\Pi_{\text{df}}^{(3)}(p^2)$ denote terms proportional to n_f and n_f^2 , respectively, with n_f being the number of active flavours. C_F refers to the Casimir operator and T_F to the trace of the fundamental representation of $SU(N)$. Because of the mass hierarchy in the quark sector only the heavy quark is considered massive whereas all lighter ($n_l = n_f - 1$) quarks are treated as massless.

Using the fact that the double fermionic contribution contains no massless cuts, $\Pi_{\text{df}}^{(3)}(p^2)$ can be expanded in a simple power series in the low energy limit $p^2 \rightarrow 0$. In the large energy limit $p^2 \rightarrow -\infty$, however, non-integer powers of p^2 arise and lead to additional logarithms of the form $\log(-p^2/m(\mu)^2)$. Thus, defining $z = p^2/4m(\mu)^2$, we end up with the expansions

$$z \rightarrow 0 : \quad \Pi_{\text{df}}^{(3)}(z) = \sum_{n>0} C_n^0(\mu) z^n, \quad (2.6)$$

$$z \rightarrow -\infty : \quad \Pi_{\text{df}}^{(3)}(z) = \sum_{n,m} C_{nm}^\infty(\mu) z^{-n} \log^m(-z). \quad (2.7)$$

3. Calculation

The basic idea for computing the full p^2 -dependence of the vacuum polarization function is to deal with massive propagator-type integrals. Although the number of integrals is moderate (approx. 10^4 for the whole four-loop contribution) they pose a challenge as far as the reduction to a small set of master integrals is concerned, since two variables, z and $d = 4 - 2\epsilon$, the dimension of space-time, are involved. For the determination of these master integrals, however, an efficient method through differential equations exists and allows for asymptotic expansions to high orders in the external momentum and high precision numerics.

In a first step all Feynman diagrams contributing to the double fermionic corrections have been projected onto scalar integrals, which were subsequently reduced to a set of 46 master integrals with the help of integration-by-parts (IBP) identities [25] and the Laporta algorithm [26] implemented in `IdSolver` [27].

To obtain the master integrals, we used the scaling property of propagator-type integrals $P_i(p^2, m^2)$

$$P_i(\lambda p^2, \lambda m^2) = \lambda^{D[P_i(p^2, m^2)]} P_i(p^2, m^2) \quad (3.1)$$

to get the characteristic differential equation

$$p^2 \frac{\partial}{\partial p^2} P_i(p^2, m^2) = -m^2 \frac{\partial}{\partial m^2} P_i(p^2, m^2) + D[P_i(p^2, m^2)] P_i(p^2, m^2) \quad (3.2)$$

with $D[P_i(p^2, m^2)]$ being the mass dimension of $P_i(p^2, m^2)$. Using relations generated from the reduction, the right hand side can again be expressed through master integrals which leads to a coupled system of inhomogeneous differential equations

$$\frac{d}{dz} P_i(z) = A_{ij}(z, \epsilon) P_j(z). \quad (3.3)$$

The matrix $A_{ij}(z, \epsilon)$ is composed of rational functions of z and ϵ . Its block-triangular form simplifies the problem to a set of several small coupled systems of differential equations and therefore provides a systematic approach to solutions of $P_i(z)$ in terms of expansions in the external momentum z (or $y = -z^{-1}$).

In the low- ($z \rightarrow 0$) and high-energy ($y \rightarrow 0$) limits, the system was solved by ansätze similar to eqns. (2.6, 2.7) for each master integral and coefficients of the series were determined recursively up to high powers in z and y , respectively.

Boundary conditions in the low energy limit are given by massive tadpole diagrams depicted in fig. 2(a), analytically calculated in [28]. In the opposite limit, all boundary conditions were determined from automatized diagrammatic large momentum expansions which lead to products of at most three loop massive tadpoles with massless propagators. Fig. 2(b) illustrates the needed propagators at the four-loop level.

The approximate linear complexity of this procedure allows for the computation of coefficients to, at least in principle, arbitrary depths. In this work, we concentrate on the first 30 and 15 terms of the expansions for $z < 1$ and $y < 1$, respectively, and are thus able to compute the master integrals in those regions with high precision.

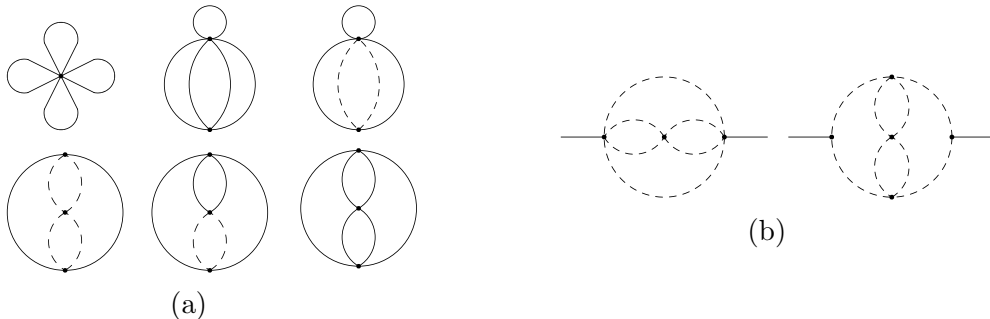


Figure 2: Boundary conditions appearing in the expansions of master integrals

In addition, an exact numerical solution of eqn. (3.3) was accomplished. For this purpose, the ϵ -expanded system of differential equations was directly integrated by means of the FORTRAN package ODEPACK [29], using the high precision values at a starting point

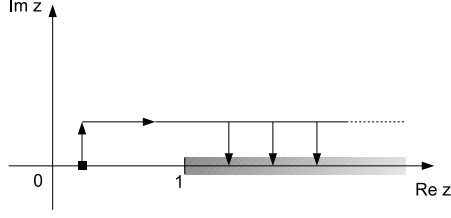


Figure 3: Integration contour chosen for the numerical integration

$|z| \ll 1$. Due to the absence of thresholds in the Euclidean domain, the numerical integration can easily be carried out along the real axis for $z < 0$. In the Minkowskian half-plane, however, (pseudo)thresholds occur and integration along the real axis is only possible below these special points. On the other hand, by virtue of contour deformation into the complex plane (see fig. 3), the master integrals can be solved numerically for arbitrary values of $z > 0$, even above $z = 1$. Variation of the integration contour is used to estimate the real achieved precision. Furthermore, the Mellin-Barnes (MB) method has been used at a few points to check the obtained values from direct integration. For this purpose, MB representations have been automatically generated with the package `MBrepresentation` [30], analytically continued in ϵ and numerically integrated with help of the MB package [31]. We observed that the high-energy expansion works very well above at least $z > 5$ and therefore the numerical integration was undertaken up to $z = 10$. This fact is also used as a cross-check of the high-energy expansion against the numerically computed polarization function.

In a last step, we performed the renormalization of the mass $m(\mu)$, the strong coupling $\alpha_s(\mu)$ and the external current in the $\overline{\text{MS}}$ -scheme.

4. Results

All analytical results for the coefficients in the small- and high-energy series in the $\overline{\text{MS}}$ -scheme up to the 30th and 15th term, respectively, are available in `Mathematica` format together with the source of this paper from <http://arxiv.org>. Apart from the new expressions at the four-loop level, we also provide so far unknown terms needed for renormalization in the large-energy expansion at the three-loop level. The Taylor series for $z \rightarrow 0$ is already known to sufficient depth [23, 24].

For the sake of clarity, here we give only the first five terms of both series at $\mathcal{O}(\alpha_s^3)$. The first coefficients in the limit $z \rightarrow 0$ are given by

$$\begin{aligned}
C_1^0 = & \frac{163868}{98415} - \frac{3287}{2430} \zeta_3 + \frac{203}{324} l_m \zeta_3 - \frac{14483}{21870} l_m + \frac{236}{3645} l_m^2 + \frac{8}{135} l_m^3 + n_l \left(\frac{262877}{262440} \right. \\
& - \frac{116}{81} a_4 - \frac{29}{486} l_2^4 + \frac{29}{486} l_2^2 \pi^2 + \frac{1421}{58320} \pi^4 - \frac{38909}{19440} \zeta_3 + \frac{203}{324} l_m \zeta_3 - \frac{3779}{21870} l_m \\
& \left. + \frac{472}{3645} l_m^2 + \frac{16}{135} l_m^3 \right) + n_l^2 \left(\frac{42173}{32805} - \frac{112}{135} \zeta_3 + \frac{1784}{3645} l_m + \frac{236}{3645} l_m^2 + \frac{8}{135} l_m^3 \right)
\end{aligned} \tag{4.1}$$

$$\begin{aligned}
C_2^0 = & \frac{1842464707}{646652160} - \frac{2744471}{1064448} \zeta_3 + \frac{14203}{27648} l_m \zeta_3 - \frac{676663}{870912} l_m - \frac{1468}{42525} l_m^2 + \frac{16}{315} l_m^3 \\
& + n_l \left(\frac{95040709}{62705664} - \frac{2029}{1728} a_4 + \frac{2029}{41472} l_2^2 \pi^2 - \frac{2029}{41472} l_2^4 + \frac{99421}{4976640} \pi^4 - \frac{12159109}{4644864} \zeta_3 \right. \\
& + \frac{14203}{27648} l_m \zeta_3 - \frac{153560977}{326592000} l_m - \frac{2936}{42525} l_m^2 + \frac{32}{315} l_m^3 \left. \right) + n_l^2 \left(\frac{15441973}{19136250} - \frac{32}{45} \zeta_3 \right. \\
& \left. + \frac{195679}{637875} l_m - \frac{1468}{42525} l_m^2 + \frac{16}{315} l_m^3 \right)
\end{aligned} \tag{4.2}$$

$$\begin{aligned}
C_3^0 = & \frac{56877138427}{12609717120} - \frac{6184964549}{1556755200} \zeta_3 + \frac{12355}{20736} l_m \zeta_3 - \frac{224445289}{244944000} l_m - \frac{310736}{4465125} l_m^2 \\
& + \frac{128}{2835} l_m^3 + n_l \left(\frac{60361465477}{29393280000} - \frac{1765}{1296} a_4 - \frac{1765}{31104} l_2^4 + \frac{1765}{31104} l_2^2 \pi^2 + \frac{17297}{746496} \pi^4 \right. \\
& - \frac{57669161}{17418240} \zeta_3 + \frac{12355}{20736} l_m \zeta_3 - \frac{37155186557}{60011280000} l_m - \frac{621472}{4465125} l_m^2 + \frac{256}{2835} l_m^3 \left. \right) \\
& + n_l^2 \left(\frac{31556642272}{49228003125} - \frac{256}{405} \zeta_3 + \frac{15480824}{52093125} l_m - \frac{310736}{4465125} l_m^2 + \frac{128}{2835} l_m^3 \right)
\end{aligned} \tag{4.3}$$

$$\begin{aligned}
C_4^0 = & \frac{270605350139987}{40351094784000} - \frac{692437613459}{119558799360} \zeta_3 + \frac{2522821}{3538944} l_m \zeta_3 - \frac{4400766606253}{4138573824000} l_m \\
& - \frac{1082216}{12629925} l_m^2 + \frac{256}{6237} l_m^3 + n_l \left(\frac{432564184014463}{165542952960000} - \frac{360403}{221184} a_4 - \frac{360403}{5308416} l_2^4 \right. \\
& + \frac{360403}{5308416} l_2^2 \pi^2 + \frac{17659747}{637009920} \pi^4 - \frac{44387709491}{10899947520} \zeta_3 + \frac{2522821}{3538944} l_m \zeta_3 - \frac{143778598477}{189621927936} l_m \\
& - \frac{2164432}{12629925} l_m^2 + \frac{512}{6237} l_m^3 \left. \right) + n_l^2 \left(\frac{667234795424}{1253204308125} - \frac{512}{891} \zeta_3 \right. \\
& \left. + \frac{1213878224}{3978426375} l_m - \frac{1082216}{12629925} l_m^2 + \frac{256}{6237} l_m^3 \right)
\end{aligned} \tag{4.4}$$

$$\begin{aligned}
C_5^0 = & \frac{1089264797862809}{114328101888000} - \frac{13766684598973}{1693749657600} \zeta_3 + \frac{1239683}{1474560} l_m \zeta_3 - \frac{9879141778777}{8136640512000} l_m \\
& - \frac{1064635136}{11345882625} l_m^2 + \frac{1024}{27027} l_m^3 + n_l \left(\frac{2680576384798219}{838813667328000} - \frac{1239683}{645120} a_4 - \frac{1239683}{15482880} l_2^4 \right. \\
& + \frac{1239683}{15482880} l_2^2 \pi^2 + \frac{8677781}{265420800} \pi^4 - \frac{1942577613953}{398529331200} \zeta_3 + \frac{1239683}{1474560} l_m \zeta_3 \\
& - \frac{580030100117579693}{644112110315520000} l_m - \frac{2129270272}{11345882625} l_m^2 + \frac{2048}{27027} l_m^3 \left. \right) \\
& + n_l^2 \left(\frac{61443753281463008}{136221219619340625} - \frac{2048}{3861} \zeta_3 + \frac{160295587080064}{511075282843125} l_m - \frac{1064635136}{11345882625} l_m^2 \right. \\
& \left. + \frac{1024}{27027} l_m^3 \right)
\end{aligned} \tag{4.5}$$

where $l_m = \log(m(\mu)^2/\mu^2)$, $l_2 = \log(2)$, $a_i = \text{Li}_i(1/2)$ with $\text{Li}_i(x)$ the polylogarithm function and ζ_i the Riemann zeta numbers.

In the limit $z \rightarrow -\infty$ we obtain

$$\begin{aligned}
C_0^\infty = & \frac{783389}{102060} - \frac{24349}{5670} \zeta_3 - \frac{20}{9} \zeta_5 + \frac{7}{24} \zeta_3 l_{xm} - \frac{113}{324} l_{xm} - \frac{1}{27} l_{xm}^2 + \frac{1}{27} l_{xm}^3 + \frac{545}{216} l_{x\mu} \zeta_3 \\
& - \frac{365}{108} l_{x\mu} - \frac{4}{9} l_{x\mu}^2 \zeta_3 + \frac{31}{54} l_{x\mu}^2 - \frac{2}{27} l_{x\mu}^3 - \frac{1}{9} l_{x\mu} l_{xm}^2 + \frac{2}{27} l_{x\mu} l_{xm} + \frac{1}{9} l_{x\mu}^2 l_{xm} \\
& + n_l \left(\frac{94735}{5832} - \frac{2855}{324} \zeta_3 - \frac{49}{4320} \pi^4 - \frac{40}{9} \zeta_5 + \frac{2}{3} a_4 + \frac{1}{36} l_2^4 - \frac{1}{36} \pi^2 l_2^2 + \frac{7}{24} l_{xm} \zeta_3 \right. \\
& - \frac{37}{324} l_{xm} - \frac{2}{27} l_{xm}^2 + \frac{2}{27} l_{xm}^3 + \frac{1153}{216} l_{x\mu} \zeta_3 - \frac{793}{108} l_{x\mu} - \frac{8}{9} l_{x\mu}^2 \zeta_3 + \frac{31}{27} l_{x\mu}^2 - \frac{4}{27} l_{x\mu}^3 \\
& - \frac{2}{9} l_{xm}^2 l_{x\mu} + \frac{4}{27} l_{xm} l_{x\mu} + \frac{2}{9} l_{xm} l_{x\mu}^2 \left. \right) + n_l^2 \left(\frac{22327}{2916} - \frac{358}{81} \zeta_3 - \frac{20}{9} \zeta_5 + \frac{19}{81} l_{xm} \right. \\
& - \frac{1}{27} l_{xm}^2 + \frac{1}{27} l_{xm}^3 + \frac{76}{27} l_{x\mu} \zeta_3 - \frac{107}{27} l_{x\mu} - \frac{4}{9} l_{x\mu}^2 \zeta_3 + \frac{31}{54} l_{x\mu}^2 - \frac{2}{27} l_{x\mu}^3 - \frac{1}{9} l_{x\mu} l_{xm}^2 \\
& \left. + \frac{2}{27} l_{x\mu} l_{xm} + \frac{1}{9} l_{x\mu}^2 l_{xm} \right) \quad (4.6)
\end{aligned}$$

$$\begin{aligned}
C_1^\infty = & \frac{16681}{1944} - \frac{38}{9} \zeta_3 + \frac{8}{3} \zeta_3 l_{x\mu} - \frac{317}{54} l_{x\mu} + \frac{13}{18} l_{x\mu}^2 - \frac{1}{9} l_{x\mu}^3 + n_l \left(\frac{10921}{972} - 4 \zeta_3 + \frac{8}{3} \zeta_3 l_{x\mu} \right. \\
& \left. - \frac{221}{27} l_{x\mu} + \frac{13}{9} l_{x\mu}^2 - \frac{2}{9} l_{x\mu}^3 \right) + n_l^2 \left(\frac{5161}{1944} + \frac{2}{9} \zeta_3 - \frac{125}{54} l_{x\mu} + \frac{13}{18} l_{x\mu}^2 - \frac{1}{9} l_{x\mu}^3 \right) \quad (4.7)
\end{aligned}$$

$$\begin{aligned}
C_2^\infty = & -\frac{7633}{9720} - \frac{571}{1620} \zeta_3 + \frac{20}{9} \zeta_5 - \frac{23}{18} \zeta_3 l_{xm} + \frac{6373}{3888} l_{xm} + \frac{355}{432} l_{xm}^2 + \frac{23}{216} l_{xm}^3 + \frac{1}{72} l_{xm}^4 \\
& + \frac{44}{27} \zeta_3 l_{x\mu} - \frac{1505}{1296} l_{x\mu} + \frac{1}{9} \zeta_3 l_{x\mu}^2 + \frac{1}{216} l_{x\mu}^2 - \frac{23}{72} l_{x\mu} l_{xm}^2 + \frac{1}{3} \zeta_3 l_{x\mu} l_{xm} - \frac{101}{54} l_{x\mu} l_{xm} \\
& + \frac{7}{24} l_{x\mu}^2 l_{xm} - \frac{1}{18} l_{x\mu} l_{xm}^3 + \frac{1}{12} l_{x\mu}^2 l_{xm}^2 - \frac{1}{18} l_{x\mu}^3 l_{xm} + n_l \left(-\frac{12733}{7776} + \frac{29}{324} \zeta_3 + \frac{1}{45} \pi^4 \right. \\
& + \frac{25}{9} \zeta_5 - \frac{1}{2} \zeta_3 l_{xm} + \frac{6113}{3888} l_{xm} + \frac{455}{432} l_{xm}^2 + \frac{43}{216} l_{xm}^3 + \frac{1}{36} l_{xm}^4 + \frac{16}{27} \zeta_3 l_{x\mu} - \frac{397}{324} l_{x\mu} \\
& + \frac{2}{9} \zeta_3 l_{x\mu}^2 + \frac{1}{108} l_{x\mu}^2 - \frac{43}{72} l_{x\mu} l_{xm}^2 + \frac{1}{3} \zeta_3 l_{x\mu} l_{xm} - \frac{257}{108} l_{x\mu} l_{xm} + \frac{7}{12} l_{x\mu}^2 l_{xm} - \frac{1}{9} l_{x\mu} l_{xm}^3 \\
& + \frac{1}{6} l_{x\mu}^2 l_{xm}^2 - \frac{1}{9} l_{x\mu}^3 l_{xm} \left. \right) + n_l^2 \left(-\frac{233}{7776} + \frac{239}{162} \zeta_3 - \frac{1}{90} \pi^4 + \frac{5}{9} \zeta_5 + \frac{7}{9} \zeta_3 l_{xm} + \frac{89}{486} l_{xm} \right. \\
& + \frac{25}{108} l_{xm}^2 + \frac{5}{54} l_{xm}^3 + \frac{1}{72} l_{xm}^4 - \frac{28}{27} \zeta_3 l_{x\mu} - \frac{83}{1296} l_{x\mu} + \frac{1}{9} \zeta_3 l_{x\mu}^2 + \frac{1}{216} l_{x\mu}^2 - \frac{5}{18} l_{x\mu} l_{xm}^2 \\
& \left. - \frac{55}{108} l_{x\mu} l_{xm} + \frac{7}{24} l_{x\mu}^2 l_{xm} - \frac{1}{18} l_{x\mu} l_{xm}^3 + \frac{1}{12} l_{x\mu}^2 l_{xm}^2 - \frac{1}{18} l_{x\mu}^3 l_{xm} \right) \quad (4.8)
\end{aligned}$$

$$\begin{aligned}
C_3^\infty = & -\frac{205123}{1049760} - \frac{593}{2430} \zeta_3 - \frac{5}{54} \zeta_3 l_{xm} + \frac{15017}{23328} l_{xm} + \frac{325}{3888} l_{xm}^2 - \frac{47}{5832} l_{xm}^3 + \frac{1}{324} l_{xm}^4 \\
& + \frac{35}{81} \zeta_3 l_{x\mu} + \frac{7963}{8748} l_{x\mu} - \frac{227}{1944} l_{x\mu}^2 + \frac{1}{36} l_{x\mu}^3 - \frac{7}{486} l_{x\mu} l_{xm}^3 + \frac{25}{648} l_{x\mu}^2 l_{xm}^2 - \frac{1}{36} l_{x\mu}^3 l_{xm} \\
& - \frac{109}{1944} l_{x\mu} l_{xm}^2 - \frac{1355}{1944} l_{x\mu} l_{xm} + \frac{283}{1944} l_{x\mu}^2 l_{xm} + n_l \left(\frac{49255}{104976} - \frac{167}{162} \zeta_3 + \frac{7}{1215} \pi^4 \right. \\
& + \frac{16}{81} \zeta_3 l_{xm} + \frac{4987}{3888} l_{xm} + \frac{3149}{11664} l_{xm}^2 + \frac{175}{5832} l_{xm}^3 + \frac{7}{972} l_{xm}^4 + \frac{23}{81} l_{x\mu} \zeta_3 + \frac{29663}{34992} l_{x\mu} \\
& - \frac{227}{972} l_{x\mu}^2 + \frac{1}{18} l_{x\mu}^3 - \frac{5}{162} l_{x\mu} l_{xm}^3 + \frac{25}{324} l_{x\mu}^2 l_{xm}^2 - \frac{1}{18} l_{x\mu}^3 l_{xm} - \frac{367}{1944} l_{x\mu} l_{xm}^2 \\
& \left. - \frac{1597}{1458} l_{x\mu} l_{xm} + \frac{283}{972} l_{x\mu}^2 l_{xm} \right)
\end{aligned}$$

$$\begin{aligned}
& + n_l^2 \left(\frac{9157}{209952} + \frac{53}{243} \zeta_3 - \frac{4}{1215} \pi^4 + \frac{59}{162} \zeta_3 l_{xm} + \frac{5905}{23328} l_{xm} + \frac{709}{5832} l_{xm}^2 + \frac{7}{243} l_{xm}^3 \right. \\
& + \frac{1}{243} l_{xm}^4 - \frac{4}{27} \zeta_3 l_{x\mu} - \frac{2189}{34992} l_{x\mu} - \frac{227}{1944} l_{x\mu}^2 + \frac{1}{36} l_{x\mu}^3 - \frac{4}{243} l_{x\mu} l_{xm}^3 + \frac{25}{648} l_{x\mu}^2 l_{xm}^2 \\
& \left. - \frac{1}{36} l_{x\mu}^3 l_{xm} - \frac{43}{324} l_{x\mu} l_{xm}^2 - \frac{2323}{5832} l_{x\mu} l_{xm} + \frac{283}{1944} l_{x\mu}^2 l_{xm} \right) \quad (4.9)
\end{aligned}$$

$$\begin{aligned}
C_4^\infty = & -\frac{35389447}{44789760} - \frac{227}{103680} \zeta_3 - \frac{895}{1728} \zeta_3 l_{xm} + \frac{2812987}{2985984} l_{xm} + \frac{125203}{248832} l_{xm}^2 + \frac{4603}{62208} l_{xm}^3 \\
& + \frac{487}{41472} l_{xm}^4 + \frac{31}{64} \zeta_3 l_{x\mu} + \frac{164053}{165888} l_{x\mu} - \frac{70553}{497664} l_{x\mu}^2 + \frac{7}{288} l_{x\mu}^3 - \frac{185}{5184} l_{x\mu} l_{xm}^3 \\
& + \frac{229}{6912} l_{x\mu}^2 l_{xm}^2 - \frac{1}{48} l_{x\mu}^3 l_{xm} - \frac{8501}{41472} l_{x\mu} l_{xm}^2 - \frac{80177}{124416} l_{x\mu} l_{xm} + \frac{2279}{20736} l_{x\mu}^2 l_{xm} \\
& + n_l \left(-\frac{19473727}{35831808} - \frac{27725}{20736} \zeta_3 + \frac{43}{6480} \pi^4 + \frac{271}{1728} \zeta_3 l_{xm} + \frac{3637091}{2985984} l_{xm} + \frac{226123}{497664} l_{xm}^2 \right. \\
& + \frac{11407}{124416} l_{xm}^3 + \frac{19}{1296} l_{xm}^4 + \frac{89}{192} l_{x\mu} \zeta_3 + \frac{47029}{41472} l_{x\mu} - \frac{70553}{248832} l_{x\mu}^2 + \frac{7}{144} l_{x\mu}^3 \\
& - \frac{497}{10368} l_{x\mu} l_{xm}^3 + \frac{229}{3456} l_{x\mu}^2 l_{xm}^2 - \frac{1}{24} l_{x\mu}^3 l_{xm} - \frac{1673}{5184} l_{x\mu} l_{xm}^2 - \frac{57629}{62208} l_{x\mu} l_{xm} \\
& \left. + \frac{2279}{10368} l_{x\mu}^2 l_{xm} \right) + n_l^2 \left(-\frac{3462161}{35831808} - \frac{745}{5184} \zeta_3 - \frac{127}{51840} \pi^4 + \frac{265}{864} \zeta_3 l_{xm} + \frac{1097}{5832} l_{xm} \right. \\
& + \frac{51077}{497664} l_{xm}^2 + \frac{2411}{124416} l_{xm}^3 + \frac{127}{41472} l_{xm}^4 - \frac{1}{48} \zeta_3 l_{x\mu} + \frac{8021}{55296} l_{x\mu} - \frac{70553}{497664} l_{x\mu}^2 \\
& + \frac{7}{288} l_{x\mu}^3 - \frac{127}{10368} l_{x\mu} l_{xm}^3 + \frac{229}{6912} l_{x\mu}^2 l_{xm}^2 - \frac{1}{48} l_{x\mu}^3 l_{xm} - \frac{4883}{41472} l_{x\mu} l_{xm}^2 \\
& \left. - \frac{35081}{124416} l_{x\mu} l_{xm} + \frac{2279}{20736} l_{x\mu}^2 l_{xm} \right) \quad (4.10)
\end{aligned}$$

with $l_{x\mu} = \log(-p^2/\mu^2)$ and $l_{xm} = \log(-p^2/m(\mu)^2)$.

In fig. 4-5 the exact result obtained from numerical integration is compared against the asymptotic behaviours of different expansion depths for Minkowskian momenta with $m = \mu$. In both regimes, we find that already a moderate number of terms reproduces the exact curve very well even close to threshold.

5. Conclusions

In this work, the low- and high-energy expansions together with an exact numerical solution of the double fermionic contribution to the heavy quark vector current correlator in four-loop approximation were obtained. We have shown that the method of differential equations provides an excellent tool to compute this quantity with high precision in the whole momentum region. Consequently, the completion of the IBP reduction represents the only remaining task to obtain the full vacuum polarization at this order.

Acknowledgements

This work was supported by the Sofja Kovalevskaja Award of the Alexander von Humboldt Foundation sponsored by the German Federal Ministry of Education and Research.

References

- [1] R. Boughezal, M. Czakon and T. Schutzmeier, Phys. Rev. D **74** (2006) 074006 [arXiv:hep-ph/0605023].
- [2] J. H. Kuhn, M. Steinhauser and C. Sturm, Nucl. Phys. B **778** (2007) 192 [arXiv:hep-ph/0702103].
- [3] R. Boughezal and M. Czakon, Nucl. Phys. B **755** (2006) 221 [arXiv:hep-ph/0606232].
- [4] K. G. Chetyrkin, M. Faisst, J. H. Kuhn, P. Maierhofer and C. Sturm, Phys. Rev. Lett. **97** (2006) 102003 [arXiv:hep-ph/0605201].
- [5] J. H. Kuhn, M. Steinhauser and T. Teubner, Phys. Rev. D **76** (2007) 074003 [arXiv:0707.2589 [hep-ph]].
- [6] F. Jegerlehner, Nucl. Phys. Proc. Suppl. **162** (2006) 22 [arXiv:hep-ph/0608329].
- [7] K. G. Chetyrkin, J. H. Kuhn and M. Steinhauser, Nucl. Phys. B **482** (1996) 213 [arXiv:hep-ph/9606230].
- [8] K. G. Chetyrkin, J. H. Kuhn and M. Steinhauser, Nucl. Phys. B **505** (1997) 40 [arXiv:hep-ph/9705254].
- [9] K. G. Chetyrkin, R. Harlander and M. Steinhauser, Phys. Rev. D **58** (1998) 014012 [arXiv:hep-ph/9801432].
- [10] K. G. Chetyrkin, J. H. Kuhn and C. Sturm, perturbative QCD,” Eur. Phys. J. C **48** (2006) 107 [arXiv:hep-ph/0604234].
- [11] K. G. Chetyrkin, A. L. Kataev and F. V. Tkachov, Phys. Lett. B **85** (1979) 277.
- [12] W. Celmaster and R. J. Gonsalves, Phys. Rev. D **21** (1980) 3112.
- [13] M. Dine and J. R. Sapirstein, Phys. Rev. Lett. **43** (1979) 668.
- [14] S. G. Gorishnii, A. L. Kataev and S. A. Larin, Phys. Lett. B **259** (1991) 144.
- [15] L. R. Surguladze and M. A. Samuel, Phys. Rev. Lett. **66** (1991) 560 [Erratum-ibid. **66** (1991) 2416].
- [16] K. G. Chetyrkin, Phys. Lett. B **391** (1997) 402 [arXiv:hep-ph/9608480].
- [17] K. G. Chetyrkin and J. H. Kuhn, Phys. Lett. B **406** (1997) 102 [arXiv:hep-ph/9609202].
- [18] K. G. Chetyrkin, R. V. Harlander and J. H. Kuhn, Nucl. Phys. B **586** (2000) 56 [Erratum-ibid. B **634** (2002) 413] [arXiv:hep-ph/0005139].
- [19] P. A. Baikov, K. G. Chetyrkin and J. H. Kuhn, Phys. Rev. Lett. **88** (2002) 012001 [arXiv:hep-ph/0108197].
- [20] P. A. Baikov, K. G. Chetyrkin and J. H. Kuhn, Phys. Lett. B **559** (2003) 245 [arXiv:hep-ph/0212303].

- [21] M. Caffo, H. Czyz, S. Laporta and E. Remiddi, *Nuovo Cim. A* **111** (1998) 365 [arXiv:hep-th/9805118].
- [22] E. Remiddi, *Nuovo Cim. A* **110** (1997) 1435 [arXiv:hep-th/9711188].
- [23] R. Boughezal, M. Czakon and T. Schutzmeier, *Nucl. Phys. Proc. Suppl.* **160** (2006) 160 [arXiv:hep-ph/0607141].
- [24] A. Maier, P. Maierhofer and P. Marquard, arXiv:0711.2636 [hep-ph].
- [25] K. G. Chetyrkin and F. V. Tkachov, *Nucl. Phys. B* **192** (1981) 159.
- [26] S. Laporta, *Int. J. Mod. Phys. A* **15** (2000) 5087 [arXiv:hep-ph/0102033].
- [27] M. Czakon, *IdSolver*, unpublished
- [28] K. G. Chetyrkin, M. Faisst, C. Sturm and M. Tentyukov, *Nucl. Phys. B* **742** (2006) 208 [arXiv:hep-ph/0601165].
- [29] Alan C. Hindmarsh: <http://www.netlib.org/odepack/>
- [30] G. Chachamis and M. Czakon, *MBrepresentation*, unpublished
- [31] M. Czakon, *Comput. Phys. Commun.* **175**, 559 (2006) [arXiv:hep-ph/0511200].

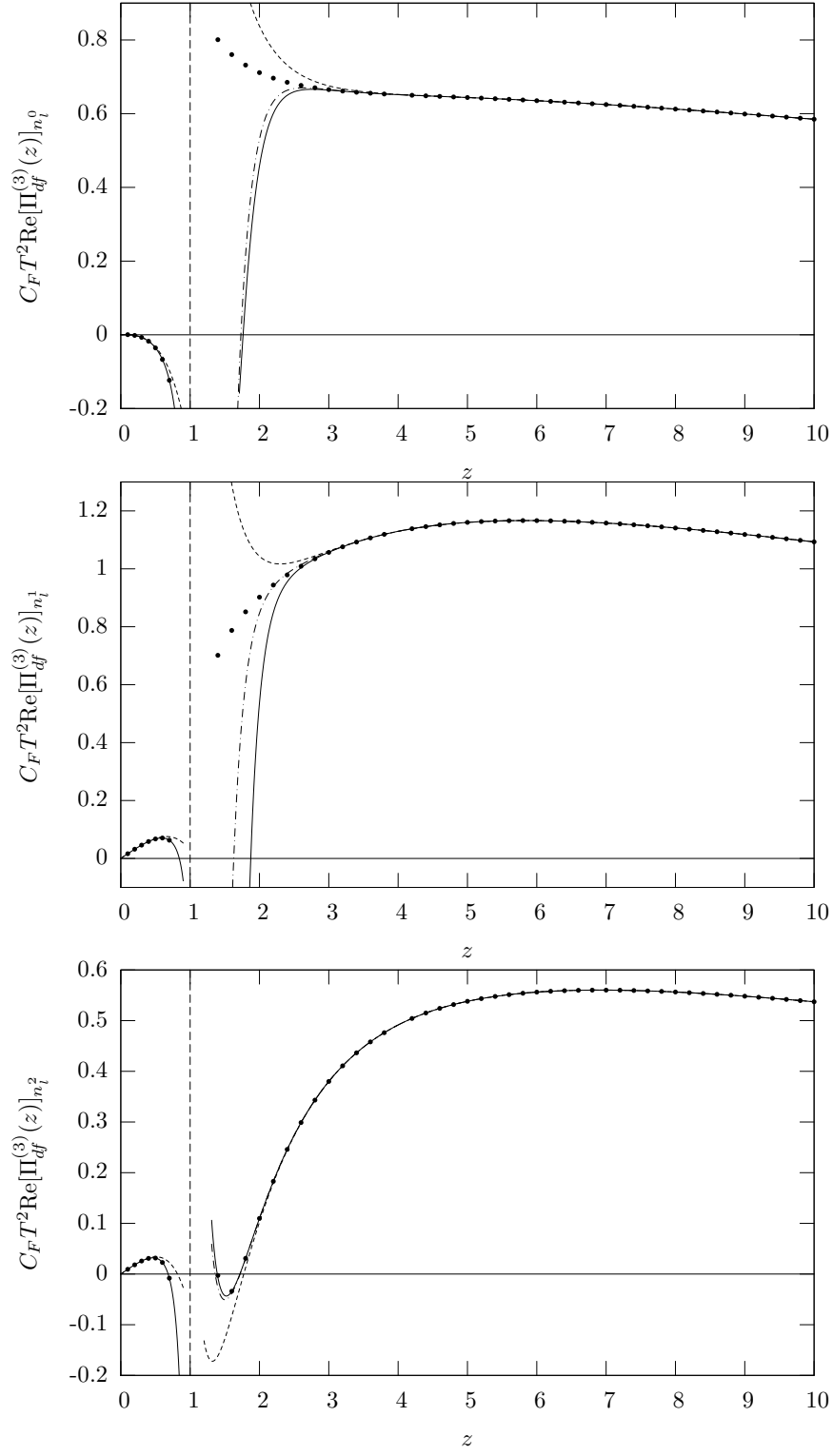


Figure 4: Comparison between expansions and numerics of the real part of $C_F T^2 \Pi_{\text{df}}^{(3)}(z)$ for each coefficient of n_l separately. Below threshold (represented by the vertical line in $z = 1$), the dashed (solid) curves correspond to low-energy expansions including the first 5 (30) terms. Above threshold the dashed, dash-dotted and solid lines denote the high-energy expansions including the first 5, 10 and 15 terms, respectively.

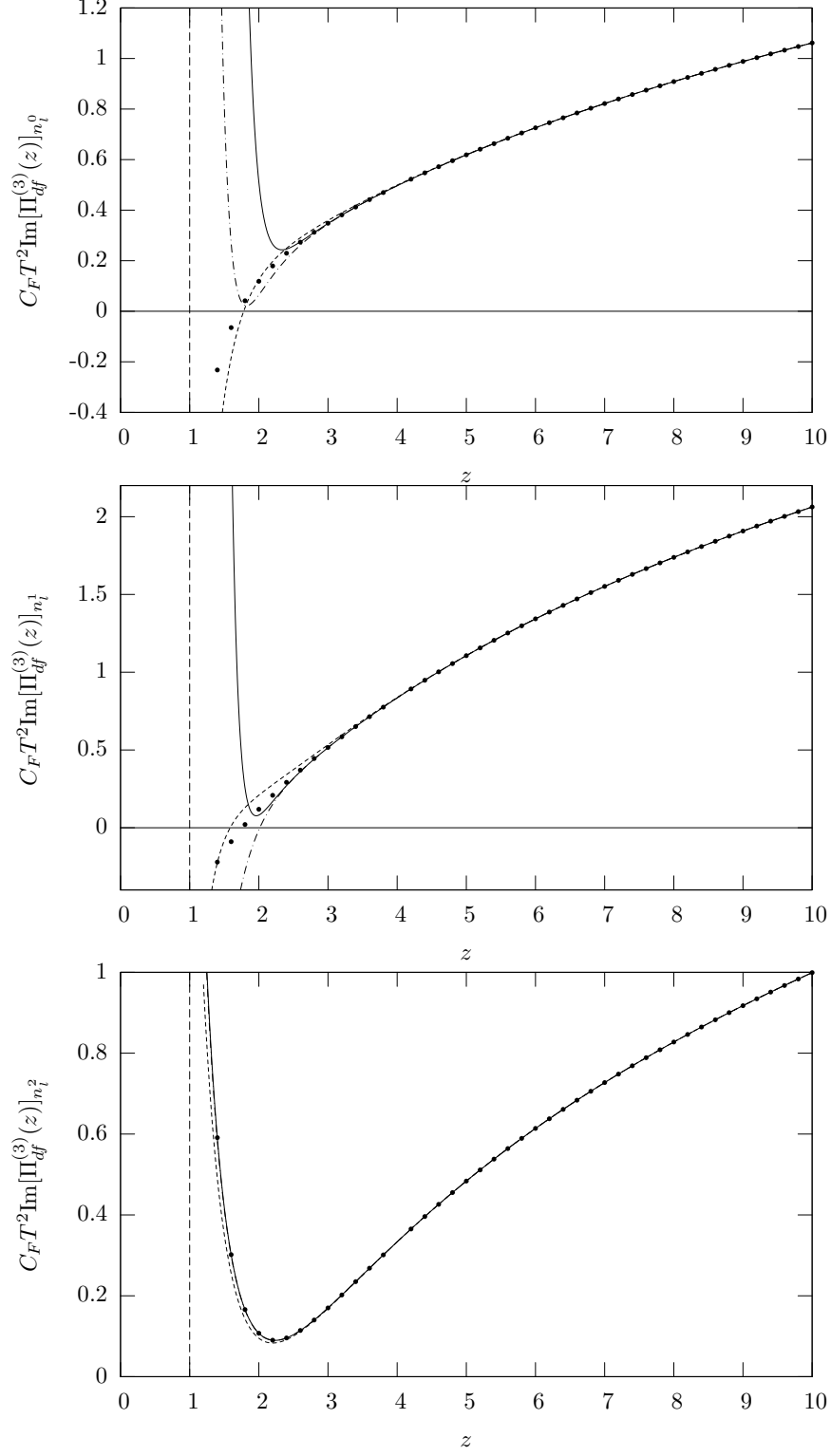


Figure 5: Comparison between expansions and numerics of the imaginary part of $C_F T^2 \Pi_{\text{df}}^{(3)}(z)$ for each coefficient of n_l separately. The dashed, dash-dotted and solid lines denote the high-energy expansions including the first 5, 10 and 15 terms, respectively.